ISBN: 978-3-95450-208-0 doi:10.18429/JACoW-IPAC2019-THPTS063

DEVELOPMENT OF A W-BAND POWER EXTRACTION STRUCTURE*

F. Toufexis†, M. Shumail, A. McGuire, B.J. Angier, D. Gamzina, S.G. Tantawi
SLAC, Menlo Park, CA94025, USA

Abstract

We are modifying the X-Band Test Accelerator at SLAC to operate as an Extreme Ultra Violet (EUV) light source. The existing photo electron gun will be replaced by a thermionic X-Band injector that utilizes RF bunch compression. The beam is accelerated up to 130 MeV using an X-Band traveling wave structure followed by a novel high shunt impedance standing wave structure. The beam then goes through a mm-wave undulator with a period of 1.75 mm, producing EUV radiation around 13.5 nm. The undulator is powered by a W-Band decelerator structure, which extracts the RF power from the electron beam. In this work we present the design and fabrication of the 91.392 GHz decelerator structure, as well as structural characterization of its cavities using SEM and 3D microscopy.

INTRODUCTION

We have designed, built, and cold-tested an RF undulator cavity operating at 91.392 GHz with an equivalent undulator period of 1.75 mm and 2.375 mm/4.92 mm input/output beam apertures [1–3]. These apertures are 5 and 10 times larger than those of a permanent magnet undulator for the same period and K value [4], and therefore this undulator could be used in a Compact 1 Å Free-Electron Laser (FEL) with a 1.4 GeV beam having several kA of peak current operating in Enhanced Self-Amplified Spontaneous Emission (E-SASE) mode [5, 6].

The RF power required at 91.392 GHz for this undulator for $K = 0.1$ is 1.4 MW. Currently the only available source of such power at these frequencies are gyrotrons with a large superconducting magnet [7, 8]. To power the undulator, we have developed a new concept for compact mm-wave sources [9]. Another method to power the undulator is to extract RF power from the drive electron beam [10] in a decelerator structure, which is the focus of this paper. We are currently designing a proof-of-concept Extreme Ultra Violet (EUV) light source driven by a thermionic RF injector [9, 11, 12] to demonstrate this approach, reusing most of the existing infrastructure of the SLAC X-Band test accelerator [13].

We developed a standing-wave parallel-coupled structure [14, 15] consisting of 40 re-entrant cavities [12, 14, 16]. The beam pipe diameter of these cavities is 340 μm and the shunt impedance is 444 $\mathrm{M\Omega\,m^{-1}}$. The power from 40 cavities is combined through two waveguide manifolds [14, 15]. The power from four such modules is further combined through another manifold, as shown in Fig. 1. We have previously reported the design of the cavities and a preliminary version of the power combining network [12, 16]. We have redesigned the power combining network for manufacturability and, at the time of this writing, we have machined several pieces of this structure. In this work we present the final RF design of the power combining manifolds, the mechanical design and manufacturing process, and preliminary structural characterization data from the cavities we have built using Scanning Electron Microscopy (SEM) and 3D microscopy.

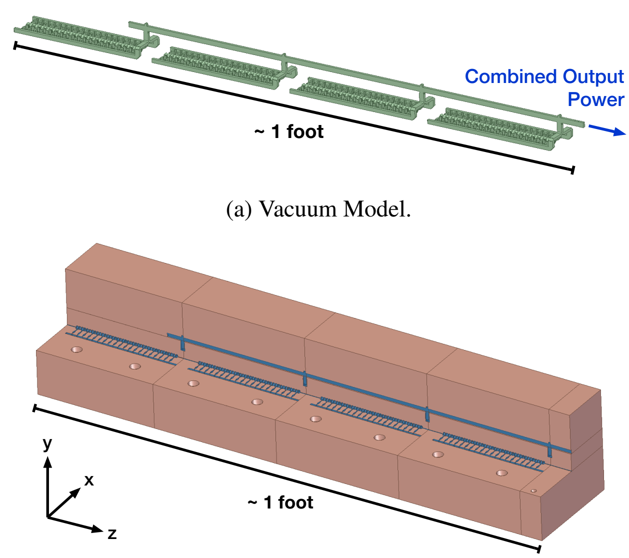

(a) Vacuum Model.

(b) Mechanical Model.

Figure 1: W-Band Power Extraction Structure.

MANIFOLD DESIGN

Two levels of manifolds combine the power of 160 cavities. The top-level manifold, shown in Fig. 2, combines the power from 4 sets of 40 cavities. An H-plane T-junction is designed using the methodology of [14, 15]. The junctions are spaced with appropriate lengths to have the same phase advance and be synchronous with the speed-of-light electron beam. The last junction is terminated with a short, positioned appropriately for the manifold to be matched. The output interface is a WR10 waveguide.

In the second manifold level, two parallel manifolds with E-plane T-junctions power-combine a total of 40 cavities (20 cavities each). The methodology of designing the T-junction 3-port network is reported in [14, 15]. When power combining 40 cavities the power going to each cavity is very small compared to the power flowing in the manifold, resulting in a waveguide height that is too thin to manufacture at these frequencies. We have redesigned the T-junctions of this manifold as shown in Fig. 3 in order to be machinable and

* This project was funded by U.S. Department of Energy under Contract No. DE-AC02-76SF00515, and the National Science Foundation under Contract No. PHY-1415437.
† ftouf@slac.stanford.edu

ISBN: 978-3-95450-208-0 doi:10.18429/JACoW-IPAC2019-THPTS063

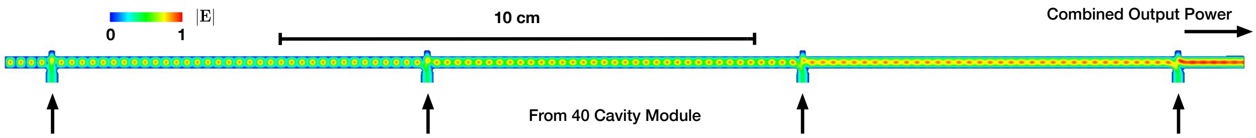

Figure 2: Electric field profile of the top-level manifold combining 4 sets of 40 cavities.

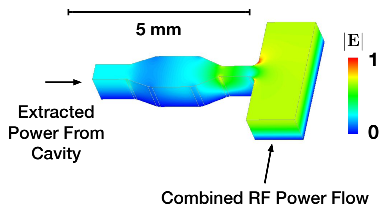

Figure 3: Electric field profile of the redesigned T-junction of the manifolds combining 20 cavities each.

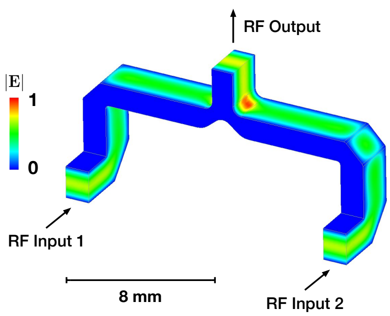

Figure 4: Electric field profile of the 3 dB combiner attached to the two bottom level manifolds, thus power-combining 40 cavities.

well-matched. Finally, the splitter/combiner of Fig. 4 power-combines the two bottom level manifolds. The combiner has been redesigned from [12, 16] to allow easy manufacturing of the overall 160-cavity decelerator structure.

MECHANICAL DESIGN & MANUFACTURING

The manufacturing of the power extraction structure was arranged in three layers in the y direction and five blocks in the z direction, as shown in Fig. 1b. Each 40-cavity module is a block, and there is a fifth capping block. The bottom layer forms the bottom half of the cavities and power combining manifolds. The middle layer forms the top half of the cavities and power combining manifolds, as well as the 3 dB combiner. The combiner is machined on the vertical side of the block, as shown in Fig. 5. The top layer forms the 4-way power combining manifold. The pieces were machined on copper silver alloy by Ron Witherspoon Inc. Once we have all the pieces, they will be cleaned/etched, and the power extraction structure will be braised and cold-tested.

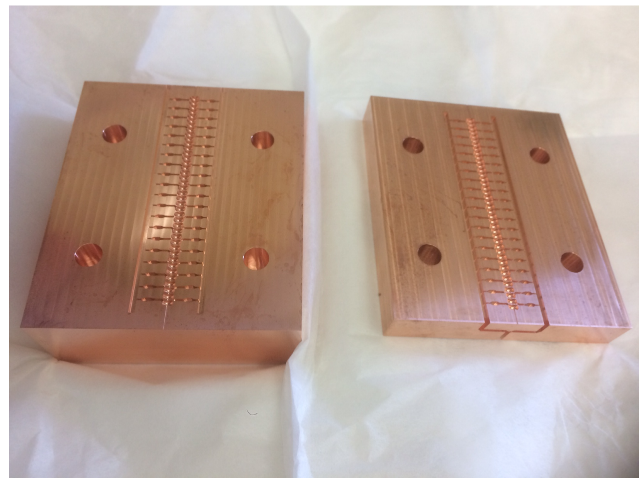

Figure 5: Picture of the bottom and middle block forming 40 cavities. Also shown is the splitter combining the two manifolds in the middle block.

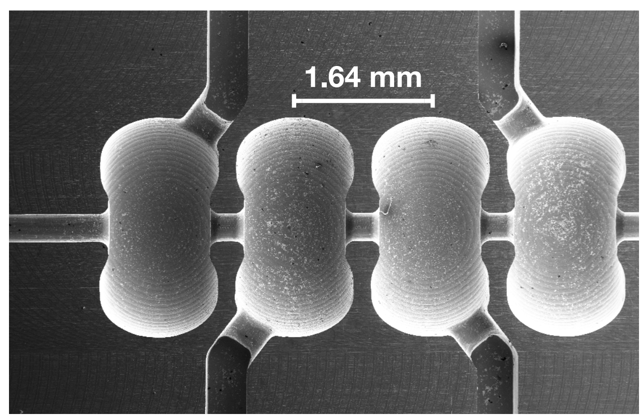

(a) Four cavities.

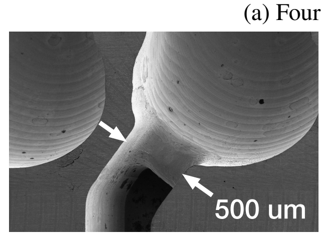

(b) Coupling hole detail.

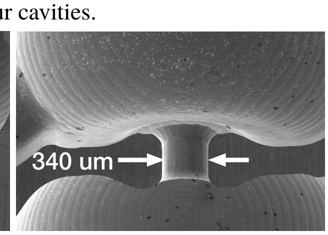

(c) Beam pipe detail.

Figure 6: SEM images of the cavities.

STRUCTURE CHARACTERIZATION

We performed SEM and 3D microscopy measurements to characterize the manufacturing process. Fig. 6 shows SEM images of the four cavities of one block. We can see the

ISBN: 978-3-95450-208-0 doi:10.18429/JACoW-IPAC2019-THPTS063

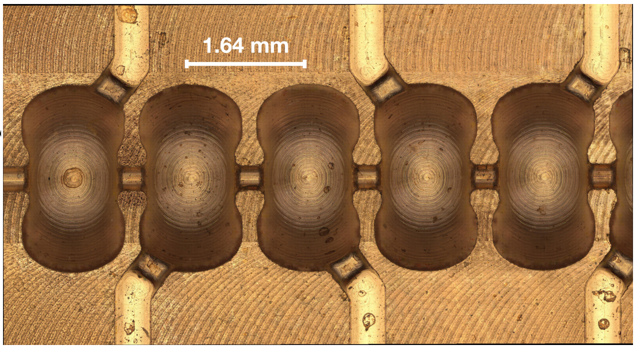

(a) 3D Microscope image of the five end cavities.

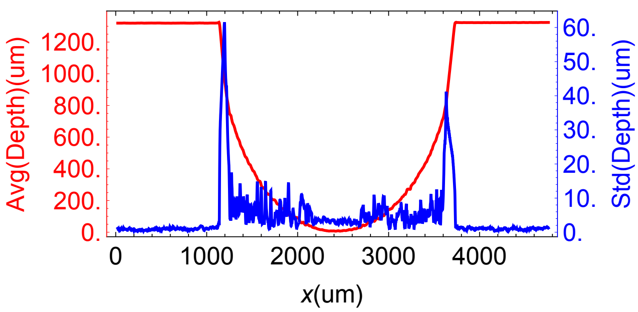

(b) Statistics of the equator cross-section of the last five cavities.

Figure 7: Nose cone profile characterization with a 3D microscope. Note that the 3D microscope can only measure depth and therefore the structure under the nose cones could not be imaged.

tool marks, but the overall finish seems adequate. Note that we typically clean and etch the structure prior to braising to improve the surface finish and remove the copper oxide.

Subsequently we characterized the structure with a 3D microscope (Keyence VK-X 1000). We took a 3D image of the end five cavities, shown in Fig. 7a. There are clearly visible tool marks and surface defects. Fig. 7b shows the average and standard deviation of the depth across the equator of the five cavities. The standard deviation at the very bottom is only a few microns but rises quickly towards the edges. Note that the process of capturing the equator is not very precise. Also there is inaccuracy measuring near vertical side walls with the 3D microscope. Note that the 3D microscope can only measure depth and therefore the structure under the nose cones could not be imaged. To obtain the profile of the nose cones we imaged the last two cell with the structure tilted about 45°. This process allows the imaging of one side of the nose cones of two cavities. Fig. 8a shows the obtained image. Fig. 8b shows a comparison between the measured and the designed nose cone profile. The measured profile very accurately follows the designed surface, except for the sharp corner at the end of the nose cone.

CONCLUSION

We have designed and are currently building a 91.392 GHz parallel-coupled power extraction structure, comprising 160 cavities that have nose cones. The aim of this structure is to provide power to an RF undulator at the same frequency having a period of 1.75 mm. We have shown the RF design of two levels of manifolds combining the power of the 160 cavities into one WR10 waveguide. We have further shown SEM and 3D microscope images characterizing the geometry and surface finish of the cavities.

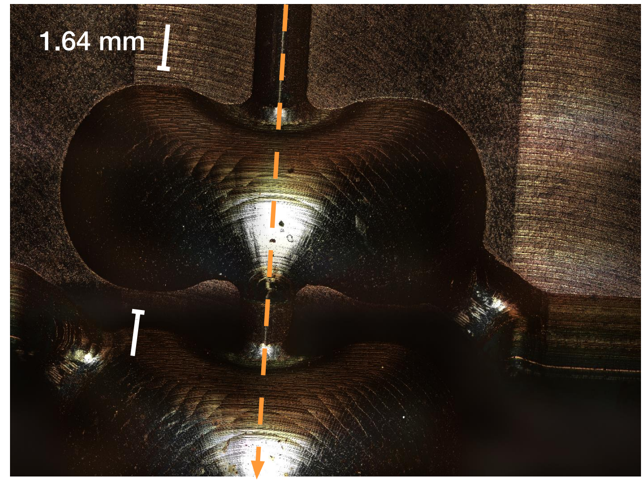

(a) 3D Microscope image of the two end cavities.

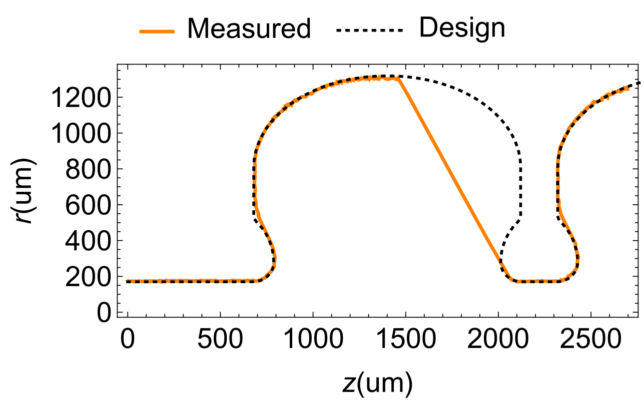

(b) Comparison of the measured nose cone profile with a 3D microscope and the design. Note that the 3D microscope can only measure depth and the structure was imaged tilted, hence only one side of the cavities could be imaged.

Figure 8: Nose cone profile characterization with a 3D microscope. Note that the image was obtained with the structure tilted, hence the poor lighting.

ACKNOWLEDGEMENTS

We wish to thank Dale Miller and Chris Pearson for their help with the structure characterization. This project was funded by U.S. Department of Energy under Contract No. DE-AC02-76SF00515, and the National Science Foundation under Contract No. PHY-1415437.

ISBN: 978-3-95450-208-0 doi:10.18429/JACoW-IPAC2019-THPTS063

REFERENCES

[1] F. Toufexis and S. G. Tantawi, "A 1.75 mm Period RF-Driven Undulator," in *Proc. 8th Int. Particle Accelerator Conf. (IPAC'17)*, Copenhagen, Denmark, May 2017, paper TUPAB135, pp. 1643–1646.

[2] F. Toufexis, J. Neilson, and S. G. Tantawi, "Coupling and Polarization Control in a mm-wave Undulator," in *Proc. 8th Int. Particle Accelerator Conf. (IPAC'17)*, Copenhagen, Denmark, May 2017, paper TUPAB136, pp. 1647–1650.

[3] F. Toufexis, D. Gamzina, and S. G. Tantawi, "Fabrication & Cold Tests of a Millimeter-Period RF Undulator," presented at Proc. 10th Int. Particle Accelerator Conf. (IPAC'19), Melbourne, Australia, May 2019, paper TUPGW098, this conference.

[4] M. Shumail, "Theory, Design, and Demonstration of a new Microwave-based Undulator," Ph.D. dissertation, Stanford University, Stanford, USA, 2014.

[5] A. A. Zholents, "Method of an enhanced self-amplified spontaneous emission for x-ray free electron lasers," *Phys. Rev. ST Accel. Beams*, vol. 8, no. 4, p. 040701, Apr. 2005.

[6] A. Zholents, "Design Considerations for the Free-Electron Laser with Self-Seeding and Current Enhanced SASE," APS, Argonne, USA, Tech. Rep. LS-335, 2013.

[7] K. L. Felch, B. G. Danly, H. R. Jory, K. E. Kreischer, W. Lawson, B. Levush, and R. J. Temkin, "Characteristics and applications of fast-wave gyrodevices," *Proceedings of the IEEE*, vol. 87, no. 5, pp. 752–781, May 1999.

[8] K. R. Chu, "The electron cyclotron maser," *Rev. Mod. Phys.*, vol. 76, no. 2, pp. 489–540, May 2004.

[9] F. Toufexis, S. G. Tantawi, A. Jensen, V. A. Dolgashev, A. Haase, M. V. Fazio, and P. Borchard, "Experimental demonstration of a 5th harmonic mm-wave frequency multiplying vacuum tube," *Applied Physics Letters*, vol. 110, no. 26, p. 263507, 2017.

[10] V. Dolgashev, "Beam Powered RF undulator," Tech. Rep., 2017.

[11] F. Toufexis, V. A. Dolgashev, C. Limborg-Deprey, and S. G. Tantawi, "A Compact Thermionic RF Injector with RF Bunch Compression fed by a Quadrupole-Free Mode Launcher," in *Proc. 8th Int. Particle Accelerator Conf. (IPAC'17)*, Copenhagen, Denmark, May 2017, paper MOPVA033, pp. 924–927.

[12] F. Toufexis, V. A. Dolgashev, C. Limborg-Deprey, and S. G. Tantawi, "A Compact EUV Light Source Using a mm-Wave Undulator", in *Proc. 8th Int. Particle Accelerator Conf. (IPAC'17)*, Copenhagen, Denmark, May 2017, pp. 928–931.

[13] C. Limborg-Deprey, C. Adolphsen, D. McCormick, M. Dunning, K. Jobe, H. Li, T. Raubenheimer, A. Vrielink, T. Vecchione, F. Wang, and S. Weathersby, "Performance of a first generation X-band photoelectron rf gun," *Phys. Rev. Accel. Beams*, vol. 19, no. 5, p. 053401, May 2016.

[14] S. G. Tantawi, Z. Li, and P. Borchard, "Distributed coupling and multi-frequency microwave accelerators," US patent no. 9,386,682, 2016.

[15] S. Tantawi, M. Nasr, Z. Li, C. Limborg, and P. Borchard, "Distributed Coupling Accelerator Structures: A New Paradigm for High Gradient Linacs," *arXiv:1811.09925*, 2018.

[16] F. Toufexis, V. A. Dolgashev, C. Limborg-Deprey, and S. G. Tantawi, "Compact linac-driven light sources utilizing mm-period RF undulators," in *Advances in Laboratory-based X-Ray Sources, Optics, and Applications VI*, G. Pareschi and A. M. Khounsary, Eds. International Society for Optics and Photonics, Aug. 2017, p. 1038704.